Pediatric Radiology (2023) 53:1049–1056
https://doi.org/10.1007/s00247-022-05574-6

ORIGINAL ARTICLE

Pilot study to determine whether reduced-dose photon-counting detector chest computed tomography can reliably display Brody II score imaging findings for children with cystic fibrosis at radiation doses that approximate radiographs

Kelly K. Horst[1] · Nathan C. Hull[1] · Paul G. Thacker[1] · Nadir Demirel[2] · Lifeng Yu[3] · Jennifer S. McDonald[3] · Nicholas B. Larson[4] · Cynthia H. McCollough[3] · Joel G. Fletcher[3]

Received: 30 August 2022 / Revised: 23 November 2022 / Accepted: 14 December 2022 / Published online: 4 January 2023

Abstract

Background The Brody II score uses chest CT to guide therapeutic changes in children with cystic fibrosis; however, patients and providers are often reticent to undergo chest CT given concerns about radiation.

Objective We sought to determine the ability of a reduced-dose photon-counting detector (PCD) chest CT protocol to reproducibly display pulmonary disease severity using the Brody II score for children with cystic fibrosis (CF) scanned at radiation doses similar to those of a chest radiograph.

Materials and methods Pediatric patients with CF underwent non-contrast reduced-dose chest PCD-CT. Volumetric inspiratory and expiratory scans were obtained without sedation or anesthesia. Three pediatric radiologists with Certificates of Added Qualification scored each scan on an ordinal scale and assigned a Brody II score to grade bronchiectasis, peribronchial thickening, parenchymal opacity, air trapping and mucus plugging. We report image-quality metrics using descriptive statistics. To calculate inter-rater agreement for Brody II scoring, we used the Krippendorff alpha and intraclass correlation coefficient (ICC).

Results Fifteen children with CF underwent reduced-dose PCD chest CT in both inspiration and expiration (mean age 8.9 years, range, 2.5–17.5 years; 4 girls). Mean volumetric CT dose index ($CTDI_{vol}$) was 0.07 ± 0.03 mGy per scan. Mean effective dose was 0.12 ± 0.04 mSv for the total examination. All three readers graded spatial resolution and noise as interpretable on lung windows. The average Brody II score was 12.5 (range 4–19), with moderate inter-reader reliability (ICC of 0.61 [95% CI=0.27, 0.84]). Inter-rater reliability was moderate to substantial for bronchiectasis (0.52), peribronchial thickening (0.55), presence of opacity (0.62) and air trapping (0.70) and poor for mucus plugging (0.09).

Conclusion Reduced-dose PCD-CT permits diagnostic image quality and reproducible identification of Brody II scoring imaging findings at radiation doses similar to those for chest radiography.

Keywords Brody II score · Children · Computed tomography · Cystic fibrosis · Lungs · Photon-counting detector computed tomography · Radiation dose

✉ Kelly K. Horst
Horst.Kelly@mayo.edu

[1] Department of Radiology, Pediatric Radiology Division, Mayo Clinic, 200 First St. SW, Rochester, MN 55905, USA

[2] Department of Pediatrics, Pediatric Pulmonology Division, Mayo Clinic, Rochester, MN, USA

[3] Department of Radiology, Mayo Clinic, Rochester, MN, USA

[4] Division of Biomedical Statistics and Informatics, Mayo Clinic, Rochester, MN, USA

Introduction

Computed tomography is considered the gold standard to display structural lung disease in children with cystic fibrosis (CF) and is more sensitive than pulmonary function tests (PFTs) and chest radiography in monitoring disease progression [1–4]. With the introduction of CF transmembrane conductance regulator modulator therapies, the new standard of care in cystic fibrosis is prevention of disease progression. Imaging strategies should therefore now include the most sensitive tools to monitor lung changes [5]. CT is noninvasive, can be performed in all ages, and serves to complement

functional data including forced expiratory volume in 1 s and the lung clearance index [5–8].

The need for routine CT imaging in children with CF necessitates optimizing low-dose CT protocols while preserving adequate spatial resolution and image contrast to maintain diagnostic accuracy. Much work has been done in the last decade to implement low-dose CT protocols to image children with CF, who are often imaged repeatedly from a very young age [9–12]. The relatively lower dose [13–18] and higher spatial resolution [15, 16, 18–21] of photon-counting detector CT (PCD-CT) compared to conventional energy integrating detector (EID) CT is particularly suited to imaging this patient population [21–23].

Photon-counting detector CT fundamentally differs from conventional EID-CT at the detector level. Conventional CT uses scintillators to convert X-rays to visible light. Reflective septae are embedded in the detectors to decrease inter-pixel scatter [21, 24] (Fig. 1). Photon-counting detectors use semiconductors to convert X-rays into electron cloud pairs, which move through a semiconductor material across a high voltage to be converted directly to signal [23, 24] (Fig. 2). The improved spatial resolution of PCD-CT compared to conventional CT is based on several resulting features: (1) Given that no septae are required between pixels in photon-counting detectors, a smaller detector pixel size can be achieved (0.18 × 0.15 mm for the NAEOTOM Alpha; Siemens Healthineers, Malvern, PA) at a higher dose efficiency [21]. The maximum spatial resolution is as high as 40 line-pairs/cm, [21] compared to up to 28 line-pairs/cm in EID-CT scanners [25]. (2) There is less optical crosstalk between detectors in PCD-CT because X-rays are not converted to visible light. (3) The direct conversion of X-rays to electronic signal in PCD-CT allows for the selective exclusion of photons below 20–25 keV, which contribute to electronic noise but not to image signal. (4) The direct conversion of X-rays to output signal in PCD-CT also allows for equal weighting of lower-energy photons, allowing for improved image contrast [21, 23, 26, 27].

Many of the detector features also reduce image noise and allow for tailored protocols that prioritize radiation dose reduction. Several studies have shown significant radiation dose reduction with PCD-CT compared to conventional CT in chest applications [28–30]. Symons et al. [28] showed lower image noise, better diagnostic quality and improved lung nodule contrast-to-noise ratio in PCD-CT over conventional CT of the chest. Jungblut et al. [29] showed that a 66% radiation dose reduction could be

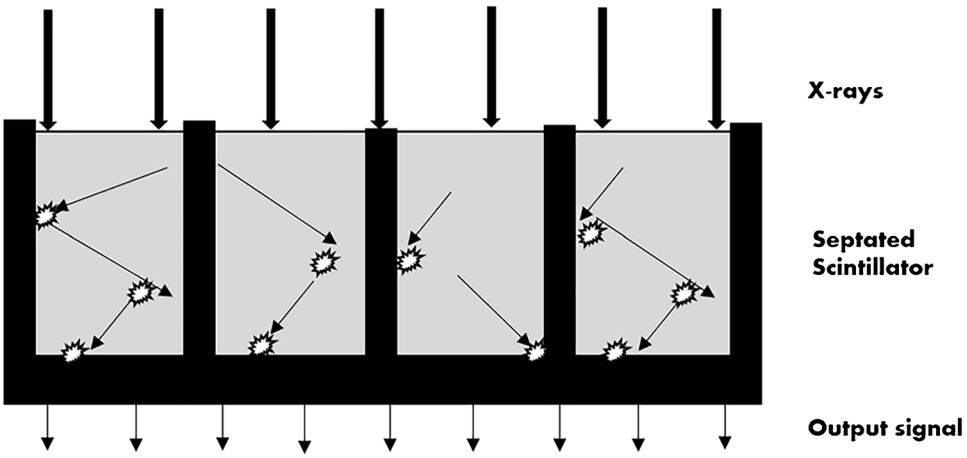

Fig. 1 Schematic of a conventional energy-integrated detector (EID) CT. A scintillator converts X-rays to visible light. The light signal is received at the photodiode, which is partitioned by reflective septae to prevent optical crosstalk between detector elements. Septae reduce the geometric dose efficiency of conventional CT

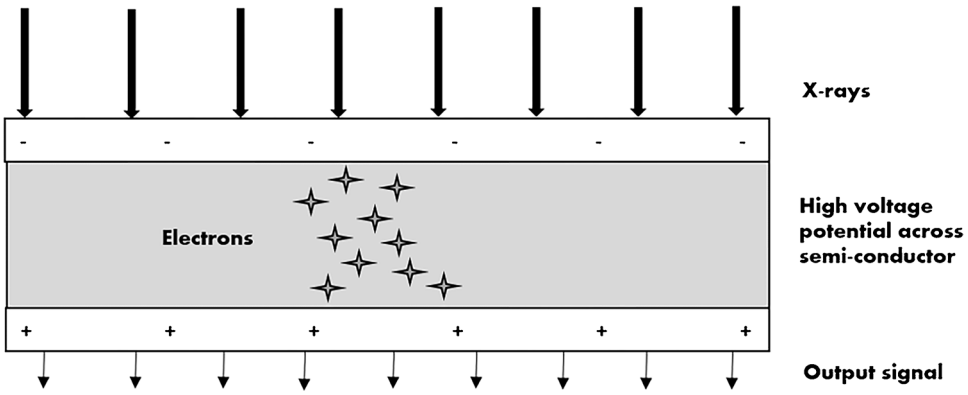

Fig. 2 Schematic illustrates the detector mechanism in photon-counting detector CT. X-rays are converted to an electron cloud that moves across a high voltage within the semiconductor. There are no septae in the detector, which allows for reduced pixel size. This translates to higher spatial resolution in CT images and greater radiation-dose efficiency of the detector

achieved without sacrificing image quality or diagnostic performance in the assessment of adult interstitial lung disease. No prior study applied PCD-CT to the imaging of pediatric patients with cystic fibrosis.

Imaging findings of CF relevant to staging the disease include elements of the Brody II scoring system: bronchiectasis, bronchial wall thickness, parenchymal opacities, air trapping and mucus plugging [5, 31]. The Brody II scoring system has been shown to correlate with PFTs, frequency of exacerbations and quality of life [6, 32, 33]. In this pilot study, we sought to determine the ability of a reduced-dose PCD chest CT protocol to reproducibly display pulmonary disease severity using the Brody II score for pediatric patients with CT scanned at radiation doses similar to those from a two-view chest radiograph.

Materials and methods

Our institutional review board approved this retrospective study. The study included pediatric patients with CF undergoing clinically indicated chest CT using our institution's reduced-dose PCD chest CT protocol, which included inspiratory and expiratory series. Waiver of informed consent was granted for this minimal risk retrospective study. We only included children who gave general consent to use medical records in research. No children were taking intravenous antibiotics at the time of imaging.

Computed tomography technique

Contiguous inspiratory and expiratory images from the lung apices to the diaphragm were obtained in each child with CF who underwent clinically indicated non-contrast reduced-dose chest PCD-CT. Images were obtained without sedation or general anesthesia. The PCD-CT system was operated in high-resolution mode, with a detector configuration of 120 × 0.2 mm. The tube potential was 100 kV with an added tin filter, rotation time was 0.25 s and helical pitch was 1.0. Axial images were reconstructed with a Qr56 reconstruction kernel, level 3 iterative reconstruction (IR) strength, 0.8-mm slice thickness, 0.5-mm slice increment and 1,024 × 1,024 matrix. A second image series was reconstructed with a Br44 kernel, level 3 IR strength, 3-mm slice thickness, 3-mm slice increment and 512 × 512 matrix.

Image review

Three pediatric radiologists with Certificates of Added Qualification (two with 10 years, K.K.H. and P.G.T., and one with 5 years of experience, N.C.H.) independently scored each scan. They assessed diagnostic image quality using ordinal rating scales, with each reader instructed to examine the entire volumetric dataset before providing any image-quality rating. Readers were further instructed to subjectively grade the spatial resolution (distal vessel and airway conspicuity) on an ordinal scale (1: unacceptable, 2: suboptimal, 3: acceptable); noise (1: cannot evaluate, 2: readable with moderate artifact, 3: readable with mild artifact, 4: no artifact); soft tissues of the mediastinum and chest wall (1: cannot evaluate, 2: readable with moderate artifact, 3: readable with mild artifact, 4: no artifact). Image-quality metrics are reported using descriptive statistics. The readers rated presence of bronchiectasis, peribronchial thickening, parenchymal opacity, air trapping and mucus plugging in each lobe of the lung using the Brody II scoring system to categorize CF severity [1]. This was done in a similar fashion to what was performed by Loeve et al. [11], who evaluated reduced-dose non-contrast conventional chest CT images in pediatric patients with CF. In short, the Brody score rates the severity of bronchiectasis and parenchymal opacification, and the extent (central vs. peripheral lung) of bronchiectasis, mucus plugging, peribronchial thickening and hyperinflation to reflect the severity of CF within the lung [1].

Statistical analysis

Image-quality metrics of spatial resolution, noise and soft-tissue evaluation are reported with mean and standard deviation. We estimated inter-rater agreement for ordinal-scaled Brody II ratings with Krippendorff alpha using the ordinal difference function, and calculated 95% confidence intervals (CIs) using percentile bootstrap intervals with 1,000 bootstrap samples, with cluster bootstrap used to account for intra-patient correlation clustering for measures involving multiple anatomical locations read per patient. We interpreted point estimates using the recommendations of Landis and Koch [34] for kappa statistics. We estimated inter-rater agreement of the Brody II scores using the intraclass correlation coefficient (ICC) along with 95% CI. Values below 0.5 indicate poor reliability, between 0.5 and 0.75 moderate reliability, between 0.75 and 0.9 good reliability, and above 0.9 excellent reliability [35].

We calculated the mean, standard deviation and range (minimum and maximum) of radiation dose of each scan in terms of volumetric CT dose index ($CTDI_{vol}$) and dose–length product (DLP). The size-specific dose estimate (SSDE) was also calculated based on the American Association of Physicists in Medicine (AAPM) task group reports 204 and 220 [36, 37]. We estimated the effective dose by multiplying the DLP by an age-specific conversion factor for the chest [38].

Results

Sixteen children were scheduled to undergo clinically indicated reduced-dose chest PCD-CT for routine clinical imaging follow-up of CF. One child could not comply with instructions during the CT examination and was excluded from the study, reducing the total number to 15 children. Four children could not breath-hold and underwent single-phase imaging. The mean age was 8.9 years (range, 2.5–17.5 years; 4 girls). The mean $CTDI_{vol}$ was 0.07 ± 0.03 mGy (minimum: 0.03 mGy, maximum 0.13 mGy) with the DLP being 1.8 ± 0.9 mGy•cm (minimum: 0.64 mGy•cm, maximum: 3.5 mGy•cm). SSDE was 0.11 ± 0.03 mGy (minimum: 0.07 mGy, maximum: 0.18 mGy) with the mean effective dose being 0.12 ± 0.04 mSv for the inspiratory and expiratory scans combined for those with two-phase imaging, a dose range that approximates that of radiographs [39–43].

Spatial resolution (distal vessel and airway conspicuity) was rated on the aforementioned 3-point scale as "acceptable" by all three readers on 13/15 scans, with two readers assessing the same scan as "suboptimal" and one reader assessing a second scan as "suboptimal" (mean, 2.93 ± 0.25). None of the scans was rated "unacceptable." All three readers assessed noise on a 4-point scale as readable with "mild" or "moderate artifact" (mean, 2.36 ± 0.56). The soft tissues were less well visualized than pulmonary structures (mean, 1.51 ± 0.78).

All three readers also scored the CT scans according to the Brody II criteria. Table 1 shows agreement among readers for each component of the Brody II score. The average Brody II score was 12.5 (range, 4–19), with moderate inter-reader reliability and ICC of 0.61 (95% CI=0.27, 0.84). Interrater reliability in terms of the Krippendorff alpha was moderate for bronchiectasis (0.52), peribronchial thickening (0.55), presence of opacity (0.62) and air trapping (0.70). Interrater reliability was poor for mucus plugging (0.09).

Figure 3 shows representative PCD-CT images from a child with CF to demonstrate the structural lung changes assessed with the Brody II criteria and to visually illustrate that these features are interpretable at radiation doses comparable to radiographs.

Figure 4 shows a side-by-side comparison of a representative PCD-CT image and an image from a conventional EID-CT obtained 16 months prior in the same girl (the same girl as shown in Fig. 3). The appearance of pulmonary structures in lung windows at 3-mm slice thickness is comparable, but the PCD-CT images were obtained at a 95% reduction in radiation dose. Figure 4 also illustrates representative axial images from the same examinations, in soft-tissue windows at similar anatomical locations at 3-mm slice thickness. There is much greater noise in the PCD-CT images. The results of our reader study attest to the limited interpretability of the soft tissues at this dose.

Table 1 Inter-rater reliability (IRR) of three readers in Brody II score assessment

Brody II criteria	IRR[a]
Bronchiectasis	0.52 (0.24–0.74)
Peribronchial thickening	0.55 (0.23–0.72)
Opacity	0.62 (–0.01–0.87)
Air trapping	0.70 (0.46–0.85)
Mucus plugging	0.09 (–0.11–0.27)

[a] As calculated using the Krippendorff alpha with bootstrapping to account for clustering (multiple locations read per patient). 95% confidence intervals are in parentheses

Figure 5 illustrates the advantages of high temporal resolution scanning utilizing two X-ray tubes in reducing patient motion. Four of the 15 children could not follow breathing commands, including the 4-year-old girl in Fig. 5. Diagnostic images were obtained despite an imperfect breath-hold.

Discussion

This pilot multi-reader study demonstrates that reduced-dose PCD-CT images obtained using high-spatial-resolution imaging in pediatric patients with CF can generate diagnostic-quality images that permit reproducible interpretation using the Brody II criteria at radiation doses that approach those of two-view chest radiographs. Using this technique, reduced-dose PCD images can be obtained in inspiration and expiration and reliably permit direct visualization and identification of bronchiectasis, peribronchial thickening, airspace opacity and air trapping. Although the absolute risks of radiation related to medical imaging in people with CF are challenging to estimate [44], the technical ability to perform CT at doses this low has significant implications for population-based imaging recommendations in people with CF, affecting up to 160,000 people worldwide [45], just under half of whom are children [46].

Imaging guidelines from the Cystic Fibrosis Foundation recommend a baseline chest radiograph within the first 3–6 months of age, once again before age 2, and every other year after age 2 [47, 48]. In pre-school-age children (ages 2–5), radiographs can be replaced with CT and be performed every 2–3 years [47, 48]. The guidelines cite *sedation* and *radiation* as the issues that combine to make the use of chest CT problematic [48]. The European Imaging Management of Cystic Fibrosis (MAESTRO) consortium cites biennial CT at radiation doses as low as reasonably achievable as the current best clinical practice [49]. PCD-CT is a new technology that is not widely available, making it

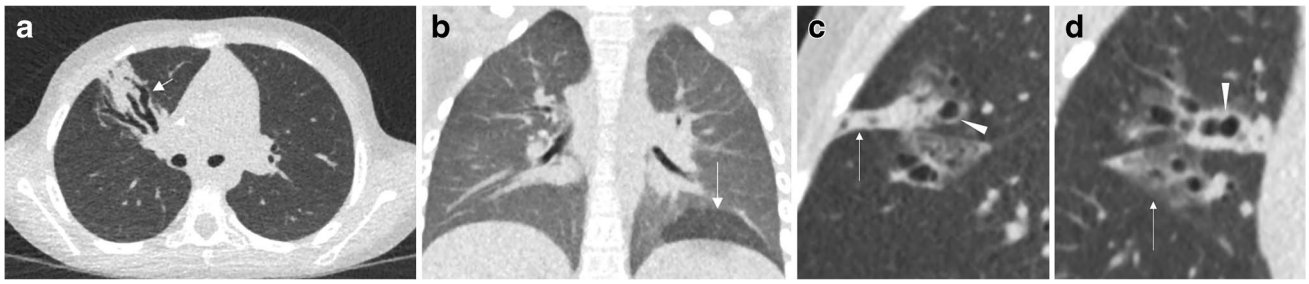

Fig. 3 Inspiratory photon-counting detector (PCD)-CT images in a 6-year-old girl with cystic fibrosis show structural lung features assessed in Brody II scoring. **a, b** Axial inspiratory image (**a**) illustrates varicose bronchiectasis (*arrow*) in the right middle lobe. Coronal expiratory image (**b**) shows air trapping (*arrow*) in the left lower lobe. **c, d** Sagittal images show mucus plugging within a dilated bronchus (*arrow* in **c**), ground-glass opacity (*arrow* in **d**) and peribronchial cuffing (*arrowhead* in **c**, **d**). Images are displayed in standard lung windows (width: 1,500; level: –500). The axial image is 0.8 mm and coronal and sagittal images are 3 mm

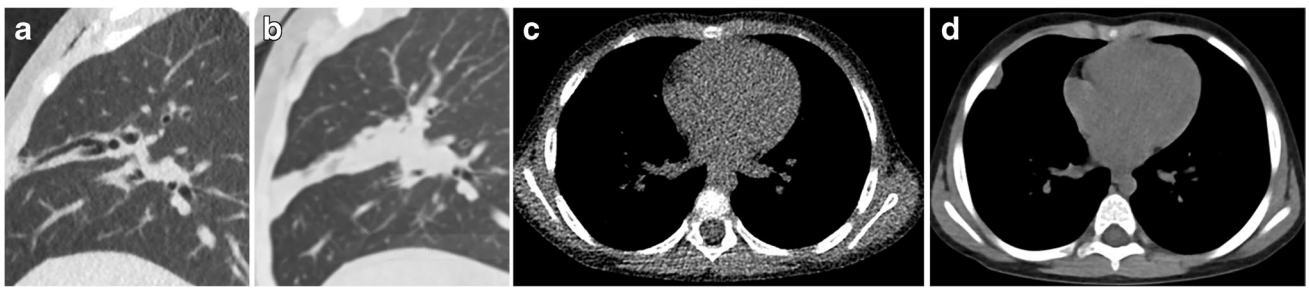

Fig. 4 Photon-counting detector (PCD)-CT images in the same 6-year-old girl with cystic fibrosis as in Fig. 3. **a–d** Lung window images show comparable image quality, despite a 95% radiation dose reduction of the PCD-CT images (**a**, sagittal) from that of the conventional energy integrating detector (EID)-CT images (**b**, sagittal. The PCD-CT volumetric CT dose index ($CTDI_{vol}$) was 0.05 mGy and the effective dose was 0.09 mSv. The EID-CT $CTDI_{vol}$ was 1.89 mGy and the effective dose was 2.2 mSv. Noise was measured in the paraspinous tissues on soft-tissue windows, at similar slices in the same child, and measured 40 Hounsfield units (HUs) on the PCD-CT image (**c**) compared to 9 HU on conventional EID-CT image (**d**). Comparison images were reconstructed with the same 3-mm slice thickness and similar reconstruction kernels

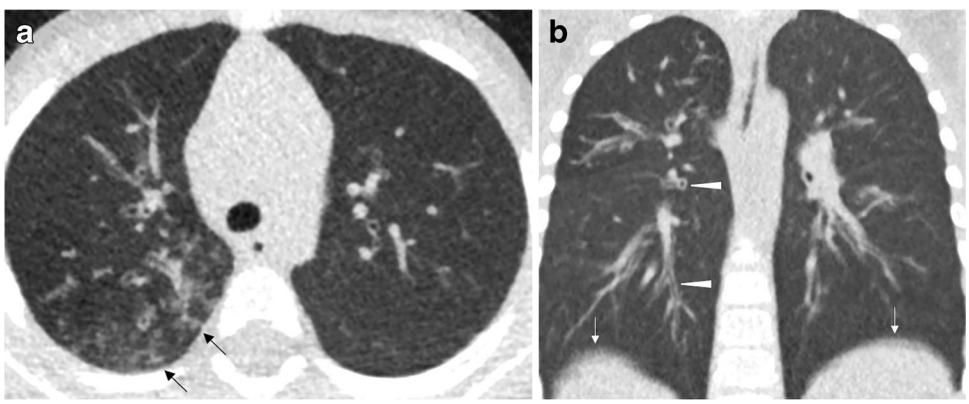

Fig. 5 Photon-counting detector (PCD)-CT images in a 4-year-old girl with cystic fibrosis. **a, b** Axial (**a**) and coronal (**b**) images at 0.8-mm slice thickness demonstrate tree-in-bud opacities in the right lower lobe (*arrows* in **a**) as well as peribronchial thickening (*arrowheads* in **b**). Some breathing motion is seen at the diaphragms (*arrows* in **b**), and these images were obtained without sedation or general anesthesia but remained diagnostic for structural lung changes of cystic fibrosis (volumetric CT dose index of 0.03 mGy; effective dose of 0.03 mSv). Readers rated this study as having "acceptable" spatial resolution, with noise levels that were "readable with moderate artifact"

difficult to be considered as the standard of care in imaging this population. However, our study does present evidence that PCD-CT can be used to stage CF with an established CT scoring system, without sedation, and at radiation doses that approach those of radiography. Subsequent to our study, technical improvements have permitted high-pitch in addition to dual-source image acquisition, which further reduces motion artifacts, particularly for pediatric patients.

All three readers assessed the spatial resolution, specifically for distal vessels and airway conspicuity, with a mean score of 2.93±0.25 on a 3-point scale, with no reader assessing any scan as "unacceptable." All three readers assessed noise levels as readable with "mild" or "moderate artifact." The scans were acceptable for assessing airways and lung parenchyma at these radiation doses; however, our results indicate that the evaluation of soft-tissue structures is limited with this technique.

In our study, the $CTDI_{vol}$ was 0.07 ± 0.03 mGy (range, 0.03–0.13 mGy) for each scan and the total effective dose was 0.12 ± 0.04 mSv for the inspiratory and expiratory scans combined. The effective dose of a standard chest radiograph depends on patient size and the number of views. Dose estimates of a single-view anteroposterior (AP) or posteroanterior (PA) chest radiograph span an estimated range of 0.007–0.014 mSv from newborns to adults, with adult lateral radiographs ranging 0.031–0.038 mSv [39]. Dose estimates for two-view pediatric chest radiographs vary widely in the literature up to 0.2 mSv, depending both on technique and methods used to calculate the effective dose [39–42].

Other studies have used reduced-dose CT in people with CF, a few of which have reported effective doses below 1 mSv [50, 51]. The radiation dose estimates achieved in our study are comparable to the effective dose of 0.04 mSv (95% confidence interval [CI]: 0.03 mSv, 0.10 mSv) published by Ernst et al. [50] and 0.08±0.01 mSv published by Moloney et al. [51], who used volumetric CT protocols performed at 80 kV with model-based iterative reconstruction to help minimize radiation dose. It would be useful to compare images from these studies directly to images obtained with a similar protocol on PCD CT.

Imaging strategies to reduce radiation in patients with CF have often included CT with intermittent slices. O'Connor et al. [10] compared 6-slice low-dose chest CT protocols at 1-mm and 0.5-mm slice-thickness in 14 pediatric patients and achieved effective dose ranges between 0.19±0.04 mSv and 0.14±0.03 mSv, respectively [10]. This is an order of magnitude lower than the dose reported in pediatric patients by Loeve et al. [11], who estimated a mean effective dose of 0.69 mSv for end-inspiratory and 0.35 mSv for end-expiratory volumetric CT, a CT protocol more comparable to our own [11].

We used the Brody II scoring system to evaluate the PCD-CT images because it represents a validated method that is applied to conventional CT images [1, 2, 31]. We report the same Brody II categories as Loeve et al. [11], with an average score of 12.5 (range, 4–19). This average score illustrates that our study consisted of children with relatively mild structural lung changes on imaging. This is not surprising given the very young age of our patient cohort, with 5 of the 15 children being age 6 years or younger. While we demonstrated moderate and acceptable reliability for the overall Brody score (ICC 0.61) and moderate to substantial agreement in all components except for mucus plugging, the interobserver agreement for mucus plugging was poor. These findings might be the result of our small population with mild and subtle disease. Other authors have examined larger cohorts with older groups of patients who had more severe manifestations of disease [52]. The purpose of our study, however, was not to validate the scoring system but to demonstrate reproducibility of the standardized scoring system using reduced-dose PCD images at a radiation dose similar to that in two-view radiographs.

Our study has multiple limitations, principally the retrospective design and the small number of children in this convenience sample. Additionally, there is no comparison to prior or concurrent imaging studies such as chest radiograph or reduced-dose EID-CT to illustrate differences using the reduced-dose PCD-CT protocol examined in this work. Further work is needed to delineate potential differences in the utility of various imaging modalities for displaying Brody II or similar imaging findings, as well as to determine whether the additional imaging findings seen on PCD-CT might change the clinical management by referring pulmonologists and improve patient outcomes.

The results of our study help illustrate how PCD-CT offers a greater degree of latitude in adjusting imaging protocols to optimize the evaluation of structural lung changes in children with CF. There are no universally agreed upon standardized CT protocols for CF [12, 49]. Intermittent slice-sampling has long been a means of radiation-dose reduction for this patient population [5, 53, 54], but structural lung changes in CF are often heterogeneous and the introduction of cystic fibrosis transmembrane conductance regulator (CFTR) modulator therapy highlights the need to track subtle changes. The ability to image whole-lung anatomy at doses comparable to those in radiographs presents new opportunities to study milder disease in younger patients. Further work is needed to determine the proper trade-offs among radiation-dose reduction, spatial and contrast resolution, and intermittent slice vs. whole lung imaging in this patient cohort.

Conclusion

This pilot study demonstrated the feasibility of performing volumetric CT in both inspiration and expiration at radiation doses that approximate radiographs to assess structural

lung changes in children with cystic fibrosis. This technical advance provides the ability to image the entire lung volume at two respiratory phases, yet also balance radiation risk and image quality.

Acknowledgments Research reported in this work was supported by the Mayo Clinic Department of Radiology and the CT Clinical Innovation Center.

Declarations

Conflicts of interest Coauthors Cynthia H. McCollough, PhD, and Joel G. Fletcher, MD, disclose a research grant to the institution from Siemens Healthcare GmbH.

References

1. Brody AS, Klein JS, Molina PL et al (2004) High-resolution computed tomography in young patients with cystic fibrosis: distribution of abnormalities and correlation with pulmonary function tests. J Pediatr 145:32–38
2. de Jong PA, Lindblad A, Rubin L et al (2006) Progression of lung disease on computed tomography and pulmonary function tests in children and adults with cystic fibrosis. Thorax 61:80–85
3. Tiddens HA, de Jong PA (2006) Update on the application of chest computed tomography scanning to cystic fibrosis. Curr Opin Pulm Med 12:433–439
4. Levy H, Kalish LA, Huntington I et al (2007) Inflammatory markers of lung disease in adult patients with cystic fibrosis. Pediatr Pulmonol 42:256–262
5. Robinson TE, Goris ML, Moss RB et al (2020) Mucus plugging, air trapping, and bronchiectasis are important outcome measures in assessing progressive childhood cystic fibrosis lung disease. Pediatr Pulmonol 55:929–938
6. Tiddens H, Andrinopoulou ER, McIntosh J et al (2020) Chest computed tomography outcomes in a randomized clinical trial in cystic fibrosis: lessons learned from the first ataluren phase 3 study. PLoS One 15:e0240898
7. Ramsey KA, Rosenow T, Turkovic L et al (2016) Lung clearance index and structural lung disease on computed tomography in early cystic fibrosis. Am J Respir Crit Care Med 193:60–67
8. Ellemunter H, Fuchs SI, Unsinn KM et al (2010) Sensitivity of lung clearance index and chest computed tomography in early CF lung disease. Respir Med 104:1834–1842
9. Joyce S, Carey BW, Moore N et al (2021) Computed tomography in cystic fibrosis lung disease: a focus on radiation exposure. Pediatr Radiol 51:544–553
10. O'Connor OJ, Vandeleur M, McGarrigle AM et al (2010) Development of low-dose protocols for thin-section CT assessment of cystic fibrosis in pediatric patients. Radiology 257:820–829
11. Loeve M, Lequin MH, de Bruijne M et al (2009) Cystic fibrosis: are volumetric ultra-low-dose expiratory CT scans sufficient for monitoring related lung disease? Radiology 253:223–229
12. Crowley C, Connor OJO, Ciet P et al (2021) The evolving role of radiological imaging in cystic fibrosis. Curr Opin Pulm Med 27:575–585
13. Zhou W, Bartlett DJ, Diehn FE et al (2019) Reduction of metal artifacts and improvement in dose efficiency using photon-counting detector computed tomography and tin filtration. Invest Radiol 54:204–211
14. Rajendran K, Voss BA, Zhou W et al (2020) Dose reduction for sinus and temporal bone imaging using photon-counting detector CT with an additional tin filter. Invest Radiol 55:91–100
15. Baffour FI, Rajendran K, Glazebrook KN et al (2022) Ultra-high-resolution imaging of the shoulder and pelvis using photon-counting-detector CT: a feasibility study in patients. Eur Radiol 32:7079–7086
16. Benson JC, Rajendran K, Lane JI et al (2022) A new frontier in temporal bone imaging: photon-counting detector CT demonstrates superior visualization of critical anatomic structures at reduced radiation dose. AJNR Am J Neuroradiol 43:579–584
17. Grunz JP, Heidenreich JF, Lennartz S et al (2022) Spectral shaping via tin prefiltration in ultra-high-resolution photon-counting and energy-integrating detector CT of the temporal bone. Invest Radiol 57:819–825
18. Leng S, Rajendran K, Gong H et al (2018) 150-mum spatial resolution using photon-counting detector computed tomography technology: technical performance and first patient images. Invest Radiol 53:655–662
19. Zhou W, Lane JI, Carlson ML et al (2018) Comparison of a photon-counting-detector CT with an energy-integrating-detector CT for temporal bone imaging: a cadaveric study. AJNR Am J Neuroradiol 39:1733–1738
20. Bartlett DJ, Koo CW, Bartholmai BJ et al (2019) High-resolution chest computed tomography imaging of the lungs: impact of 1,024 matrix reconstruction and photon-counting detector computed tomography. Invest Radiol 54:129–137
21. Rajendran K, Petersilka M, Henning A et al (2022) First clinical photon-counting detector CT system: technical evaluation. Radiology 303:130–138
22. Rajendran K, Petersilka M, Henning A et al (2021) Full field-of-view, high-resolution, photon-counting detector CT: technical assessment and initial patient experience. Phys Med Biol 66(20)
23. Rajendran K, Marsh J, Petersilka M et al (2021) High resolution, full field-of-view, whole body photon-counting detector CT: system assessment and initial experience. Proc SPIE Int Soc Opt Eng 11595:115950D
24. Leng S, Bruesewitz M, Tao S et al (2019) Photon-counting detector CT: system design and clinical applications of an emerging technology. Radiographics 39:729–743
25. Kawashima H, Ichikawa K, Takata T, Seto I (2022) Comparative assessment of noise properties for two deep learning CT image reconstruction techniques and filtered back projection. Med Phys 49:6359–6367
26. Flohr T, Petersilka M, Henning A et al (2020) Photon-counting CT review. Phys Med 79:126–136
27. Gutjahr R, Halaweish AF, Yu Z et al (2016) Human imaging with photon counting-based computed tomography at clinical dose levels: contrast-to-noise ratio and cadaver studies. Invest Radiol 51:421–429
28. Symons R, Pourmorteza A, Sandfort V et al (2017) Feasibility of dose-reduced chest CT with photon-counting detectors: initial results in humans. Radiology 285:980–989
29. Jungblut L, Euler A, von Spiczak J et al (2022) Potential of photon-counting detector CT for radiation dose reduction for the assessment of interstitial lung disease in patients with systemic sclerosis. Invest Radiol 57:773–779
30. Graafen D, Emrich T, Halfmann MC et al (2022) Dose reduction and image quality in photon-counting detector high-resolution computed tomography of the chest: routine clinical data. J Thorac Imaging 37:315–322
31. Brody AS, Kosorok MR, Li Z et al (2006) Reproducibility of a scoring system for computed tomography scanning in cystic fibrosis. J Thorac Imaging 21:14–21
32. Goralski JL, Stewart NJ, Woods JC (2021) Novel imaging techniques for cystic fibrosis lung disease. Pediatr Pulmonol 56:S40–S54
33. Zorzo C, Caballero P, Diab L et al (2020) Predictive value of computed tomography scoring systems evolution in adults with cystic fibrosis. Eur Radiol 30:3634–3640

34. Landis JR, Koch GG (1977) The measurement of observer agreement for categorical data. Biometrics 33:159–174
35. Koo TK, Li MY (2016) A guideline of selecting and reporting intraclass correlation coefficients for reliability research. J Chiropr Med 15:155–163
36. Boone J, Strauss K, Cody D et al (2011) Size-specific dose estimates (SSDE) in pediatric and adult body CT examinations. Report of AAPM Task Group 204. American Association of Physicists in Medicine, College Park
37. McCollough C, Bakalyar DM, Bostani M et al (2014) Use of water equivalent diameter for calculating patient size and size-specific dose estimates (SSDE) in CT: the report of AAPM Task Group 220. AAPM Rep 2014:6–23
38. Romanyukha A, Folio L, Lamart S et al (2016) Body size-specific effective dose conversion coefficients for CT scans. Radiat Prot Dosimetry 172:428–437
39. Wall BF, Kendall GM, Edwards AA et al (2006) What are the risks from medical X-rays and other low dose radiation? Br J Radiol 79:285–294
40. McCollough C, Cody D, Edyvean S et al (2008) The measurement, reporting, and management of radiation dose in CT. Report of AAPM Task Group 23. American Association of Physicists in Medicine, College Park
41. Lahham A, Issa A (2021) Evaluation of radiation doses in pediatric patients undergoing conventional chest X-ray examination. Health Phys 120:212–216
42. Shatskiy IG, Ivanov D, Reznik VA et al (2021) Doses and radiation risk of the chest X-ray examination of children with COVID-19. American Institute of Physics, St. Petersburg
43. American College of Radiology (2022) Radiation dose to adults from common imaging examinations. RadiologyInfo.org. https://www.acr.org/-/media/ACR/Files/Radiology-Safety/Radiation-Safety/Dose-Reference-Card.pdf. Accessed 5 Dec 2022
44. Kuo W, Ciet P, Tiddens HA et al (2014) Monitoring cystic fibrosis lung disease by computed tomography. Radiation risk in perspective. Am J Respir Crit Care Med 189:1328–1336
45. Guo J, Garratt A, Hill A (2022) Worldwide rates of diagnosis and effective treatment for cystic fibrosis. J Cyst Fibros 21:456–462
46. Knapp EA, Fink AK, Goss CH et al (2016) The Cystic Fibrosis Foundation patient registry. Design and methods of a national observational disease registry. Ann Am Thorac Soc 13:1173–1179
47. Lahiri T, Hempstead SE, Brady C et al (2016) Clinical practice guidelines from the Cystic Fibrosis Foundation for preschoolers with cystic fibrosis. Pediatrics 137:e20151784
48. Foundation CF, Borowitz D, Robinson KA et al (2009) Cystic Fibrosis Foundation evidence-based guidelines for management of infants with cystic fibrosis. J Pediatr 155:S73–S93
49. Ciet P, Bertolo S, Ros M et al (2022) State-of-the-art review of lung imaging in cystic fibrosis with recommendations for pulmonologists and radiologists from the "Imaging Management of Cystic Fibrosis" (MAESTRO) consortium. Eur Respir Rev 31:21073
50. Ernst CW, Basten IA, Ilsen B et al (2014) Pulmonary disease in cystic fibrosis: assessment with chest CT at chest radiography dose levels. Radiol 273:597–605
51. Moloney F, Kavanagh RG, Ronan NJ et al (2021) Ultra-low-dose thoracic CT with model-based iterative reconstruction (MBIR) in cystic fibrosis patients undergoing treatment with cystic fibrosis transmembrane conductance regulators (CFTR). Clin Radiol 76:393.e9–393.e17
52. de Jong PA, Tiddens HA (2007) Cystic fibrosis specific computed tomography scoring. Proc Am Thorac Soc 4:338–342
53. de Jong PA, Nakano Y, Lequin MH, Tiddens HA (2006) Dose reduction for CT in children with cystic fibrosis: is it feasible to reduce the number of images per scan? Pediatr Radiol 36:50–53
54. Jimenez S, Jimenez JR, Crespo M et al (2006) Computed tomography in children with cystic fibrosis: a new way to reduce radiation dose. Arch Dis Child 91:388–390